

# Chitosan-derived nitrogen-doped carbon-bearing Brønsted acid sites as a green catalyst for the C–C bond-forming coupling of chalcone with malononitrile

Duong Trinh The Anh<sup>1,2</sup>, Nguyen Truong Hai<sup>1,2,\*</sup>



Use your smartphone to scan this QR code and download this article

<sup>1</sup>Department of Organic Chemistry, Faculty of Chemistry, University of Science, Ho Chi Minh City, Vietnam

<sup>2</sup>Vietnam National University-Ho Chi Minh City, Ho Chi Minh City, Vietnam

## Correspondence

**Nguyen Truong Hai**, Department of Organic Chemistry, Faculty of Chemistry, University of Science, Ho Chi Minh City, Vietnam

Vietnam National University-Ho Chi Minh City, Ho Chi Minh City, Vietnam

Email: ngthai@hcmus.edu.vn

## History

- Received: 30-09-2025
- Revised: 18-12-2025
- Accepted: 19-01-2026
- Published Online: 18-06-2026

## DOI :

<https://doi.org/10.32508/vnuhcmj-std.v29i2.4612>



## Copyright

© VNUHCM Journal. This is an open-access article distributed under the terms of the Creative Commons Attribution 4.0 International license.

## ABSTRACT

A nitrogen-doped carbon catalyst was systematically prepared via a green-chemistry route, using chitosan as an accessible yet reusable biopolymeric precursor. The preparative procedure involved pyrolyzing chitosan under an inert atmosphere at 550 °C, enabling efficient incorporation of nitrogen functionalities into the resulting carbon matrix. Subsequently, a surface modification involved the incorporation of –SO<sub>3</sub>H groups to furnish the catalyst with a substantial number of Brønsted acidic sites. The incorporation of acidic functionalities together with nitrogen-rich domains is significant. This combination results in a bifunctional surface capable of simultaneously activating both nucleophilic and electrophilic species, broadening the scope of catalytic transformations. The catalytic efficiency of the catalyst was examined using the Michael addition reaction, using chalcone and malononitrile as representative substrates. Under mild conditions (40 °C for 2 h), the catalyst efficiently drove the reaction to produce the corresponding adduct with yields up to 70%. Hence, a synergistic effect between nitrogen and Brønsted acidic sites is necessary to activate bonds and stabilize the transition state to promote reactivity and selectivity. Beyond its catalytic effectiveness, this work highlights the importance of developing green, reusable heterogeneous catalysts from biomass. This approach not only reduces systemic reliance on precious and toxic metal-based systems but also enhances the usability of natural biopolymers, such as chitosan. These previously wasted materials can be rendered useful as catalytic agents. Altogether, this work provides an environmentally friendly and flexible approach to developing carbon-based acid catalysts.

**Key words:** Brønsted acid, nitrogen-doped, chalcone, chitosan, green catalyst

## INTRODUCTION

Heterogeneous catalysts exhibiting robust acidity have received significant interest in recent years, to the extent that they are replacing classical homogeneous acid catalysts, such as H<sub>2</sub>SO<sub>4</sub>, *p*-TSA, and HCl. This replacement is due to the characteristic merits of heterogeneous catalysts, viz., easy recoverability, metered dosage, reusability with minimal loss of catalytic activity, and low risk and reduced environmental hazards<sup>1</sup>.

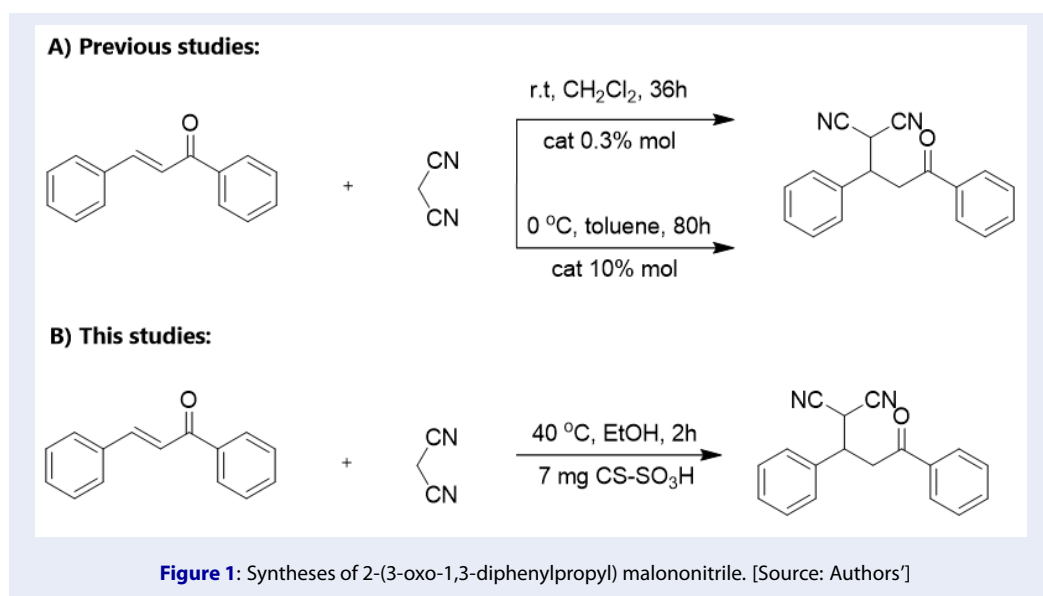
Following the trend toward sustainable development, biomass sources and agricultural residues have emerged as valuable feedstocks for fabricating functional materials. Various studies have investigated the conversion of biomass into useful carbon-based products, such as graphitic carbon nitride (*g*-C<sub>3</sub>N<sub>4</sub>)<sup>2,3</sup>, carbon quantum dots (CQDs)<sup>4</sup>, and graphene oxide<sup>5</sup>. Among these promising precursors, chitosan appears particularly significant given its availability and its ability to be converted natively into nitrogen-doped carbon-based materials. About 6–8 million

tons of chitin-containing waste per annum are estimated to be generated from crab, shrimp, and shell residues, forming a readily available feedstock for chitosan production<sup>6</sup>.

Chitosan is a natural polysaccharide derived from chitin, the second most abundant carbon-based polymer after cellulose. To obtain chitosan, chitin is usually subjected to depolymerization and deacetylation in a 40%–50% alkaline solution at 100–160 °C for 1–3 hours<sup>7</sup>. With its relatively high nitrogen content (approximately 7 wt%) and functional moieties such as acetamide and amine groups, chitosan is a good precursor for nitrogen-rich carbon materials<sup>8</sup>.

Carbon-based materials from chitosan have potential uses in environmental remediation, biomedicine, and catalysis. The pyrolysis of chitosan at 550 °C under an inert N<sub>2</sub> flow was used to produce nitrogen-doped carbon. The availability of nitrogen functionalities on the carbon skeleton promoted sulfonation in the next step, boosting the introduction of –SO<sub>3</sub>H functionalities on the surface.

**Cite this article :** Anh D T T, Hai N T. Chitosan-derived nitrogen-doped carbon-bearing Brønsted acid sites as a green catalyst for the C–C bond-forming coupling of chalcone with malononitrile. *VNUHCMJ. Sci. Technol. Dev.* 2026; 29(2):4105-4119.



Beyond facilitating the anchoring of  $-\text{SO}_3\text{H}$  groups, nitrogen doping introduces electronic heterogeneity, defect sites, and enhanced surface polarity, which collectively improve sulfonation efficiency, acidity, and catalytic performance. In particular, pyridinic and pyrrolic nitrogen species provide intrinsic acid–base sites and promote substrate adsorption and activation. Additionally, nitrogen dopants modulate charge distribution within the carbon framework, strengthening interactions with polar reactants and synergistically enhancing catalytic activity when combined with  $-\text{SO}_3\text{H}$  groups. This work presents a new synthesis of N-doped sulfonated carbon via the high-temperature pyrolysis of chitosan ( $550\text{ }^\circ\text{C}$ ) followed by hydrothermal sulfonation using *p*-toluenesulfonic acid. This route is fundamentally different from previously reported one-step hydrothermal or diazonium-based sulfonation strategies<sup>9–11</sup>. The resulting sulfonated nitrogen-doped carbon was used as a heterogeneous catalyst for the organic conversion of chalcone to malononitrile. The conversion time decreased compared to previous works. In addition, the catalyst was easy to recover and highly reusable. The physicochemical properties of the material were carefully elucidated using modern techniques, i.e., Fourier transform infrared, XRD, SEM, and EDS Figure 1.

## MATERIALS AND METHODS

### Chemicals

Benzaldehyde ( $\geq 99\%$ ) was obtained from Merck, USA. 4-Fluorobenzaldehyde ( $\geq 98.49\%$ ) was purchased from Bidepharm, Shanghai, China, and 4-

bromobenzaldehyde ( $\geq 99\%$ ) from Leyan, China. 4-Methylbenzaldehyde ( $\geq 97\%$ ), 4-chlorobenzaldehyde ( $\geq 98\%$ ), and 4'-nitroacetophenone ( $> 98\%$ ) were purchased from Merck (Germany). Chitosan ( $\geq 90\%$ ), *p*-TSA ( $\geq 99\%$ ), citric acid ( $\geq 99\%$ ), lactic acid ( $\geq 85\%$ ), and sodium hydroxide (NaOH) ( $\geq 96\%$ ) were obtained from Xilong, China. Additionally, the common methanol ( $\geq 99.5\%$ ), ethanol ( $\geq 99.5\%$ ), acetonitrile ( $\geq 99\%$ ), acetone ( $\geq 95\%$ ), ethyl acetate ( $\geq 99.5\%$ ), toluene ( $\geq 99.5\%$ ), chloroform ( $\geq 99\%$ ), diethyl ether ( $\geq 99.5\%$ ), and *n*-hexane ( $\geq 99\%$ ) were supplied by Chemsol, Vietnam. Malononitrile was obtained from Sigma-Aldrich.

### Analytical techniques

X-ray diffraction (XRD) analysis was carried out using a Rigaku MiniFlex 300/600 diffractometer equipped with a D/teX Ultra 1D detector and a  $\text{CuK}\alpha$  radiation source ( $\lambda_1 = 1.54059\text{ \AA}$ ,  $\lambda_2 = 1.54441\text{ \AA}$ ) (XRD; Rigaku Corporation, Japan). Scanning electron microscopy (SEM) images were obtained using a field-emission scanning electron microscope (FE-SEM; Merlin, Carl Zeiss, Germany) equipped with an InLens detector, operated at an accelerating voltage of 10.00 kV and a working distance of 4.3 mm. SEM combined with energy-dispersive X-ray spectroscopy (EDS) was used to examine the morphology and elemental composition of the samples, with SEM imaging performed at  $10,000\times$  magnification and an accelerating voltage of 20 kV. At the same time, EDS spectra were acquired using a live time of approximately 20 seconds to detect C, O, N, and S. The working distance and tilt angle were optimized to enhance signal

quality during elemental mapping. Fourier transform infrared (FTIR) spectra were recorded using a Bruker E400 FTIR spectrometer (Ettlingen, Germany). Nuclear magnetic resonance measurements ( $^1\text{H-NMR}$  and  $^{13}\text{C-NMR}$ ) were performed on a Bruker Avance 500 MHz spectrometer, with  $\text{CDCl}_3$  and  $\text{DMSO-}d_6$  serving as both solvent and internal standard.

### Synthesis of nitrogen-doped carbon materials with Brønsted acid sites from chitosan (CS-SO<sub>3</sub>H)

The resulting CS-SO<sub>3</sub>H catalyst was prepared using the two-step method. Initially, pyrolysis was performed on chitosan under an inert N<sub>2</sub> atmosphere at 550 °C for 4 h. After that, the chitosan was treated with acid in the presence of citric acid and *p*-TSA. The step was performed in the Teflon-lined autoclave for 4 h at 160 °C. After washing with deionized water and drying under reduced pressure at 100 °C, the end product was obtained as a black solid (Figure 2). The physicochemical properties and the purity of the resultant product were characterized using FT-IR spectroscopy, XRD, EDS, and SEM.

### Synthesis of chalcone

Chalcones were synthesized via the Claisen-Schmidt condensation using aryl-aldehydes and acetophenones as substrates in EtOH/NaOH at room temperature. Upon completion, the reaction mixture was cooled and poured into crushed ice, yielding the desired chalcone product. The crude product was subsequently recrystallized from EtOH to obtain the pure compound<sup>12</sup>.

### Synthesis of 2-(3-oxo-1,3-diphenylpropyl)malononitrile

In a typical procedure, (2*E*)-1,3-diphenylprop-2-en-1-one (1 mmol) was reacted with malononitrile (1 mmol) in ethanol (3 mL) in the presence of CS-SO<sub>3</sub>H as the catalyst at 40 °C under continuous stirring for 120 min. The progress of the reaction was monitored by thin-layer chromatography (TLC). After completion, the mixture was cooled to room temperature, and the catalyst was separated. The resulting product was recrystallized from ethanol (10–15 mL). The obtained compound was characterized by  $^1\text{H}$  and  $^{13}\text{C}$  NMR spectroscopy.

**2-(3-Oxo-1,3-diphenylpropyl)malononitrile (1a).** (2*E*)-1,3-diphenylprop-2-en-1-one (208 mg), malononitrile (66 mg), CS-SO<sub>3</sub>H (7 mg). The white solid was isolated with 70% yield (188.6 mg).  $R_f = 0.52$  (*n*-hexane:EA=8:2);  $^1\text{H-NMR}$  (500 MHz,  $\text{CDCl}_3$ ):

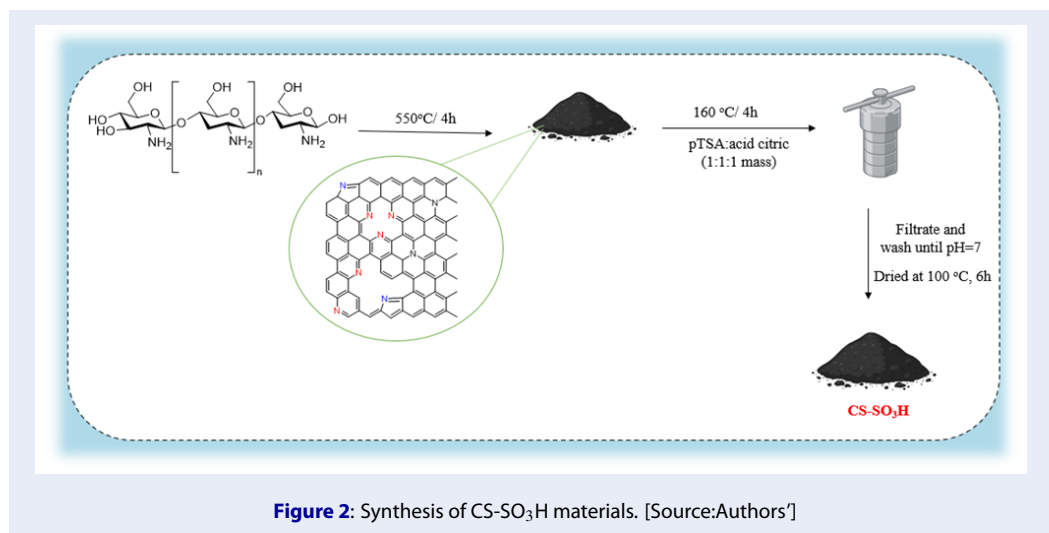
$\delta = 3.67$  (s, 2H), 3.96 (s, 1H), 4.65 (s, 1H), 7.54 (m, 8H), 7.97 (s, 2H) ppm.  $^{13}\text{C-NMR}$  (125 MHz,  $\text{CDCl}_3$ ):  $\delta = 28.8, 40.1, 41.2, 111.7, 111.8, 128.0, 128.1, 128.9, 129.2, 129.4, 134.2, 135.8, 136.5$  ppm.

**2-(1-(4-Fluorophenyl)-3-oxo-3-phenylpropyl)malononitrile (1b).** (2*E*)-3-(4-fluorophenyl)-1-phenylprop-2-en-1-one (226.3 mg), malononitrile (66 mg), CS-SO<sub>3</sub>H (7 mg). The white solid was isolated with 31% yield (90.3 mg).  $R_f = 0.48$  (*n*-hexane:EA=8:2);  $^1\text{H-NMR}$  (500 MHz,  $\text{DMSO-}d_6$ ):  $\delta = 3.66$  (dd,  $J = 18.0, 5.5$  Hz, 1H), 3.86 (dd,  $J = 18.0, 8.5$  Hz, 1H), 4.12 (dt,  $J = 8.5, 6.0$  Hz, 1H), 5.24 (d,  $J = 6.0$  Hz, 1H), 7.09 (q,  $J = 16.0$  Hz, 1H), 7.23 (t,  $J = 9.0$  Hz, 2H), 7.54 (q,  $J = 15.0$  Hz, 3H), 7.66 (t,  $J = 7.5$  Hz, 1H), 8.00 (d,  $J = 7.0$  Hz, 2H) ppm.  $^{13}\text{C-NMR}$  (125 MHz,  $\text{DMSO-}d_6$ ):  $\delta = 29.3, 39.6, 40.3, 113.1, 113.4, 115.5$  (d,  $J = 21.3$  Hz), 128.1, 128.8, 130.4 (d,  $J = 8.4$  Hz), 133.6, 134.0 (d,  $J = 3.0$  Hz), 136.0, 161.9 (d,  $J = 243.0$  Hz), 196.3 ppm.

**2-(1-(4-Chlorophenyl)-3-oxo-3-phenylpropyl)malononitrile (1c).** (2*E*)-3-(4-chlorophenyl)-1-phenylprop-2-en-1-one (242.7 mg), malononitrile (66 mg), CS-SO<sub>3</sub>H (7 mg). The white solid was isolated with 45% yield (137.5 mg).  $R_f = 0.48$  (*n*-hexane:EA=8:2);  $^1\text{H-NMR}$  (500 MHz,  $\text{DMSO-}d_6$ ):  $\delta = 3.66$  (dd,  $J = 18.5, 5.5$  Hz, 1H), 3.88 (dd,  $J = 18.0, 8.5$  Hz, 1H), 4.12 (dt,  $J = 8.5, 6.0$  Hz, 1H), 5.25 (d,  $J = 6.0$  Hz, 1H), 7.46 (dd,  $J = 8.5, 2.0$  Hz, 2H), 7.53 (m, 4H), 7.66 (t,  $J = 7.5$  Hz, 1H), 7.99 (dd,  $J = 8.5, 1.0$  Hz, 2H) ppm.  $^{13}\text{C-NMR}$  (125 MHz,  $\text{DMSO-}d_6$ ):  $\delta = 29.1, 39.7, 40.1, 113.1, 113.3, 128.1, 128.6, 128.8, 130.2, 132.9, 133.7, 136.0, 136.9, 196.3$  ppm.

**2-(1-(4-Bromophenyl)-3-oxo-3-phenylpropyl)malononitrile (1d).** (2*E*)-3-(4-bromophenyl)-1-phenylprop-2-en-1-one (287.2 mg), malononitrile (66 mg), CS-SO<sub>3</sub>H (7 mg). The white solid was isolated with 26% yield (86.3 mg)  $R_f = 0.48$  (*n*-hexane:EA=8:2);  $^1\text{H-NMR}$  (500 MHz,  $\text{DMSO-}d_6$ ):  $\delta = 3.66$  (dd,  $J = 18.0, 5.5$  Hz, 1H), 3.87 (dd,  $J = 18.0, 8.5$  Hz, 1H), 4.10 (dt,  $J = 8.5, 6.0$  Hz, 1H), 5.25 (d,  $J = 6.5$  Hz, 1H), 7.46 (d,  $J = 8.5$  Hz, 2H), 7.53 (t,  $J = 8.0$  Hz, 2H), 7.60 (d,  $J = 8.5$  Hz, 2H), 7.66 (t,  $J = 7.5$  Hz, 1H), 7.98 (d,  $J = 7.5$  Hz, 2H).  $^{13}\text{C-NMR}$  (125 MHz,  $\text{DMSO-}d_6$ ):  $\delta = 29.0, 39.7, 40.1, 113.0, 113.3, 121.6, 128.1, 128.8, 130.5, 131.5, 133.7, 136.0, 137.3, 196.3$  ppm.

**2-(1-(4-methylphenyl)-3-oxo-3-phenylpropyl)malononitrile (1e).** (2*E*)-3-(4-methylphenyl)-1-phenylprop-2-en-1-one (222.3 mg), malononitrile (66 mg), CS-SO<sub>3</sub>H (7 mg). The white solid was isolated with 32% yield (87.6 mg).  $R_f = 0.63$  (*n*-hexane:EA=8:2);  $^1\text{H-NMR}$  (500 MHz,



DMSO-*d*<sub>6</sub>):  $\delta$  = 2.17 (s, 3H), 4.21 (dd,  $J$  = 12.0, 2.5 Hz, 1H), 4.48 (d,  $J$  = 12.0 Hz, 1H), 4.67 (s,  $J$  = 12.0 Hz, 1H), 5.68 (s, 1H), 6.95 (t,  $J$  = 7.5 Hz, 1H), 7.08 (m, 2H), 7.26 (m, 2H), 7.39 (d,  $J$  = 8.0 Hz, 2H), 7.51 (q,  $J$  = 8.0 Hz, 2H) ppm.

#### 2-(3-(4-nitrophenyl)-3-oxo-1-

phenylpropyl)malononitrile (1f). (2*E*)-1-(4-nitrophenyl)-1-phenylprop-2-en-1-one (253.3 mg), malononitrile (66 mg), CS-SO<sub>3</sub>H (7 mg). The yellow solid was isolated with 60% yield (191.1 mg).  $R_f$  = 0.25 (*n*-hexane:EA=8:2); <sup>1</sup>H-NMR (500 MHz, DMSO-*d*<sub>6</sub>):  $\delta$  = 4.30 (d,  $J$  = 13.0 Hz, 1H), 4.59 (d,  $J$  = 12.0 Hz, 1H), 4.85 (d,  $J$  = 12.0 Hz, 1H), 6.34 (s, 1H), 7.32 (t,  $J$  = 7.5 Hz, 2H), 7.47 (t,  $J$  = 7.5 Hz, 1H), 7.67 (m, 3H), 7.88 (m, 3H) ppm.

#### Catalyst recovery process

After completion of the reaction, the solid catalyst was isolated and sequentially washed with ethanol (10 × 5 mL) and acetone (10 × 5 mL). This procedure eliminated residual components from the reaction mixture, and the success of the process was confirmed using TLC. The catalyst was activated for subsequent reactions by drying the material at 100 °C for 2 h. The reusability of the catalyst was investigated under optimized conditions, with consecutive runs extended to 5 cycles.

#### Procedure for conducting the leaching test

A reaction mixture containing (2*E*)-1,3-diphenylprop-2-en-1-one (3 mmol), malononitrile (3 mmol), CS-SO<sub>3</sub>H (21 mg), and EtOH (9.0 mL) was stirred magnetically at 40 °C. After 60 min, the mixture was divided into three portions: In

portion I, CS-SO<sub>3</sub>H was separated from the reaction mixture, followed by recrystallization of the product in ethanol (5–10 mL). In portion II, CS-SO<sub>3</sub>H was taken out after 60 min, and the remaining reaction was subjected to magnetic stirring for an additional 60 min. Upon completion, the mixture was crystallized from ethanol. In portion III, the reaction mixture was allowed to proceed for another 60 min with magnetic agitation. After completion, CS-SO<sub>3</sub>H was removed, and the resulting mixture was crystallized from ethanol (5–10 mL).

## RESULTS AND DISCUSSION

### Catalytic properties

The structure and surface chemistry of the CS-SO<sub>3</sub>H material were studied with Fourier transform infrared spectroscopy (FT-IR), XRD, SEM, and energy-dispersive X-ray spectroscopy (EDX).

The FT-IR spectrum of the chitosan sample (Figure 3 (a)) exhibited characteristic absorption bands at 3440 cm<sup>-1</sup> corresponding to -OH and -NH<sub>2</sub> groups, 2925 cm<sup>-1</sup> assigned to Csp<sup>3</sup>-H stretching, 1654 cm<sup>-1</sup> attributed to the bending vibration of -NH<sub>2</sub>, 1321 cm<sup>-1</sup> corresponding to C-N stretching, and at 1154 and 1556 cm<sup>-1</sup> ascribed to amide groups. These features are consistent with the structure of pristine chitosan. For the chitosan sample calcined at 550 °C (Figure 3 (b)), the absorption bands in the range of 3400–3000 cm<sup>-1</sup> disappeared after pyrolysis, indicating the transformation of the -OH and -NH<sub>2</sub> groups. Additionally, a distinct C-O-C stretching band appeared at 1253 cm<sup>-1</sup>. In the sample prepared with CS-SO<sub>3</sub>H (Figure 3 (c)), a broad absorption band was observed at 3323 cm<sup>-1</sup>, corresponding to the -OH

group, along with signals at 1162 and 1214  $\text{cm}^{-1}$  assigned to S=O stretching, and a band at 662  $\text{cm}^{-1}$  characteristic of O=S=O vibrations. These results confirm the successful sulfonation of the material.

The XRD pattern of the obtained material (Figure 4) exhibits a peak at  $2\theta \approx 24^\circ$ , which corresponds to the (002) plane of graphite, in agreement with JCPDS card No. 89-8487. In addition, the relatively broad baseline indicates low crystallinity and a significant amorphous character, which is consistent with the SEM observations.

The SEM images in Figure 5 indicate that the synthesized material lacks a well-defined morphology; instead, it aggregates into elongated rod-like structures and irregular bulk forms. The surface is characterized by a dense distribution of pores with non-uniform sizes, which can facilitate mass transfer and improve the accessibility of active sites during catalytic reactions.

Moreover, the elemental mapping shown in Figure 6 confirms the successful sulfonation of the material, as sulfur atoms are homogeneously dispersed across the surface. This uniform distribution of sulfur functionalities is expected to increase the number of Brønsted acid sites, enhancing the catalytic performance. The combined effect of porous morphology and well-dispersed acidic groups underscores the potential of this material to act as an efficient heterogeneous catalyst.

EDS analysis showed that the synthesized catalyst contains 52.99 wt% C, 30.50 wt% O, 15.56 wt% N, and 0.95 wt% S. The corresponding atomic percentages were determined to be 58.12% C, 28.68% O, 12.81% N, and 0.39% S (Figure 7).

### Synthesis of 2-(3-oxo-1,3-diphenylpropyl)malononitrile

The catalytic performance of CS-SO<sub>3</sub>H was assessed using the reaction between chalcone and malononitrile to prepare (1a). Here, a systematic study of the effect of various reaction parameters on product yield was performed by varying parameters, such as the use of the catalytic sulfonic acid CS-SO<sub>3</sub>H and the reaction temperature (Figure 8).

A solution containing chalcone (1 mmol) and malononitrile (1 mmol) was treated for varied time intervals (60, 90, 120, 180, 240, 300, and 360 min) at 40 °C in the presence of CS-SO<sub>3</sub>H (10 mg) using EtOH as the solvent (entries 8–13, Table 1). From Table 1, the reaction yield increased over time, reaching a maximum at 120 min, after which it decreased, indicating

that the product yield is significantly affected by reaction time. The reaction was then prolonged to examine the effect of temperature (RT, 40, 60, 80, 100, 120, and 140 °C) (entries 1–7, Table 1). The yield was maximal at 51% at 40 °C. In addition, the effects of solvent volume and catalyst loading on the yield were investigated. The conversion between chalcone and malononitrile had a 52% yield in the absence of any catalyst, whereas the yield increased to 70% when 7 mg of CS-SO<sub>3</sub>H was used with 3 mL of EtOH.

To investigate the catalytic performance of CS-SO<sub>3</sub>H, the reaction between chalcone and malononitrile to give (1a) was conducted at 40 °C for 120 min in EtOH with various catalysts (Table 2). The catalysts selected for comparison with CS-SO<sub>3</sub>H were *p*-TSA, HCl, H<sub>2</sub>SO<sub>4</sub>, citric acid, lactic acid, and acetic acid; these are all acids. Apart from H<sub>2</sub>SO<sub>4</sub> (yield 17%), the reactions did not proceed. One potential reason for this is the reduced amount of H<sup>+</sup> ions to promote catalytic action. Chitosan (CS) was also used as a catalyst in the reaction to assess the specific contribution of the -SO<sub>3</sub>H groups. In general, when compared to CS and nitrogen-doped carbon (pyrolyzed CS) (Table 2, entries 7–9), CS-SO<sub>3</sub>H was significantly more active as a catalyst. To further evaluate the catalytic performance of CS-SO<sub>3</sub>H, g-C<sub>3</sub>N<sub>4</sub>-SO<sub>3</sub>H was used as a comparative catalyst under identical reaction conditions. In this case, the reaction proceeded with a markedly lower yield of only 10%, indicating that g-C<sub>3</sub>N<sub>4</sub>-SO<sub>3</sub>H exhibits substantially lower catalytic activity than CS-SO<sub>3</sub>H for this transformation (Table 2, entry 17). Importantly, entry 16 (Table 2) indicates that using CS-SO<sub>3</sub>H in solvent gave a larger yield than when the reaction was performed in the absence of solvent (entry 10). This reduction in yield can be attributed to the crystallization of the product during the reaction, which inhibited contact between the substrate and catalyst on a molecular level. The role of the solvent was further confirmed: the yield of the reaction improved progressively as the polarity increased from non-polar to polar; the greatest yield occurred when EtOH was used as the reaction medium (entries 10–15, Table 2).

The reaction between chalcone and malononitrile was carried out at 40 °C in 3 mL of EtOH using CS-SO<sub>3</sub>H as the catalyst with different substrate ratios (1:1, 1:1.5, 1:2, and 1.5:1) to determine the optimal conditions. As shown in Table 3, the chalcone-to-malononitrile ratio of 1:1 produced the highest yield.

From Figure 9, the reaction between malononitrile and chalcone derivatives catalyzed by CS-SO<sub>3</sub>H in ethanol under reflux at 40 °C resulted in a series of 2-(3-oxo-1,3-diphenylpropyl)malononitrile

**Table 1: Influence of reaction parameters on product (1a) yield.<sup>a</sup>[Source:Authors']**

Entry	Temp. (°C)	Time (min)	Amount (mg)	V <sub>solvent</sub> (mL)	Yield <sup>b</sup> (%)
1	RT	360	10	3	39
2	40	360	10	3	51
3	60	360	10	3	46
4	80	360	10	3	44
5	100	360	10	3	43
6	120	360	10	3	38
7	140	360	10	3	26
8	40	60	10	3	53
9	40	90	10	3	53
10	40	120	10	3	66
11	40	180	10	3	56
12	40	240	10	3	43
13	40	300	10	3	41
14	40	120	0	3	52
15	40	120	1	3	39
16	40	120	3	3	42
17	40	120	5	3	49
18	40	120	7	3	70
19	40	120	10	3	66
20	40	120	15	3	58
21	40	120	20	3	51
22	Microwave	10	10	3	33 <sup>c</sup>
23	Ultrasonic	120	10	3	64 <sup>d</sup>
24	40	120	10	0	38
25	40	120	10	1	41
26	40	120	10	5	63
27	40	120	10	7	53
28	40	120	10	10	50

<sup>a</sup>Reaction condition: Chalcone (1 mmol), malononitrile (1 mmol), and CS-SO<sub>3</sub>H (10 mg) in EtOH.  
<sup>b</sup>Isolated yield through crystallization in EtOH (10–15 mL).  
<sup>c</sup>Microwave irradiation (80 W) and CS-SO<sub>3</sub>H (10 mg) in EtOH (3 mL).  
<sup>d</sup>The ultrasonic method at 40 °C within 2 h using CS-SO<sub>3</sub>H (10 mg) in EtOH (3 mL).

**Table 2: Influence of different catalysts and solvents on reaction efficiency.<sup>a</sup> [Source: Authors']**

Entry	Catalyst	Solvent	Yield <sup>b</sup> (%)
1	<i>p</i> -TSA <sup>c</sup>	EtOH	Trace
2	HCl <sup>d</sup>	EtOH	Trace
3	H <sub>2</sub> SO <sub>4</sub> <sup>e</sup>	EtOH	17
4	Citric acid	EtOH	Trace
5	Lactic acid	EtOH	Trace
6	CH <sub>3</sub> COOH <sup>f</sup>	EtOH	Trace
7	Chitosan (merchandise)	EtOH	57
8	Calcined Chitosan	EtOH	62
9	CS-SO <sub>3</sub> H	MeOH	53
10	CS-SO <sub>3</sub> H	EtOH	66
11	CS-SO <sub>3</sub> H	DMSO	46
12	CS-SO <sub>3</sub> H	Acetonitrile	53
13	CS-SO <sub>3</sub> H	Chloroform	15
14	CS-SO <sub>3</sub> H	Ethyl acetate	22
15	CS-SO <sub>3</sub> H	Toluene	22
16	CS-SO <sub>3</sub> H	Solvent-free	38
17	g-C <sub>3</sub> N <sub>4</sub> -SO <sub>3</sub> H <sup>g</sup>	EtOH	10

<sup>a</sup>Reaction condition: Chalcone (1 mmol), malononitrile (1 mmol) and CS-SO<sub>3</sub>H (10 mg) in EtOH.  
<sup>b</sup>Isolated yield through crystallization in EtOH (10–15 mL).  
<sup>c</sup>10 mg of *p*-TSA.  
<sup>d</sup>8.5 mL of HCl (37.0 wt% in water).  
<sup>e</sup>5.4 mL of H<sub>2</sub>SO<sub>4</sub> (98.0 wt% in water).  
<sup>f</sup>9.5 mL of CH<sub>3</sub>COOH.  
<sup>g</sup>7 mg g-C<sub>3</sub>N<sub>4</sub>-SO<sub>3</sub>H.

**Table 3: Investigation into impact of substrate proportion on reaction yield.<sup>a</sup> [Source: Authors']**

Entry	Chalcone (mmol)	Malononitrile (mmol)	Isolated yield <sup>b</sup> (%)
1	1	1	67
2	1	1.5	66
3	1	2	65
4	1.5	1	62

<sup>a</sup>Reaction condition: (2E)-1,3-diphenylprop-2-en-1-one (1 mmol), malononitrile (1 mmol) and CS-SO<sub>3</sub>H (10 mg) in 3 mL of EtOH at 40 °C.  
<sup>b</sup>Isolated yield through crystallization in EtOH (10–15 mL).

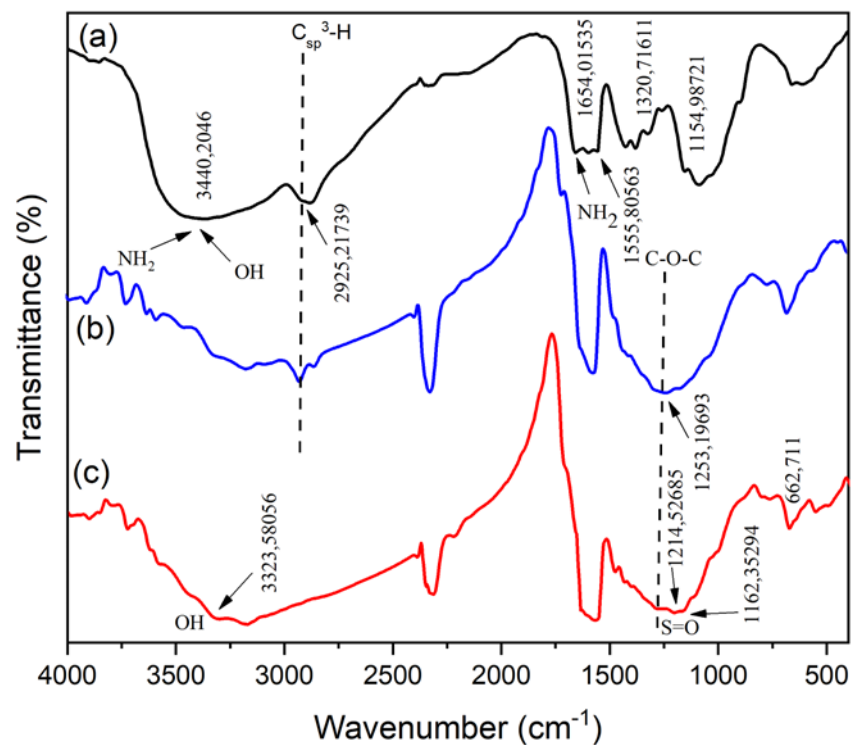


Figure 3: FT-IR spectra of (a) chitosan, (b) calcined chitosan at 550 °C, and (c) CS-SO<sub>3</sub>H. [Source: Authors']

derivatives with moderate to good yields. Under the established optimal conditions, the scope of synthesizing 2-(3-oxo-1,3-diphenylpropyl)malononitrile derivatives using (2*E*)-1,3-diphenylprop-2-en-1-one with malononitrile with a magnetic stirrer was also examined. A range of (2*E*)-1,3-diphenylprop-2-en-1-one derivatives bearing either electron-withdrawing group (*e.g.*, 4-F, 4-Cl, and 4-Br) and electron-donating substituents (*e.g.*, 4-Me) proved compatible with this transformation, although the desired products were isolated in modest yields. However, the yield of 2-(3-(4-nitrophenyl)-3-oxo-1-phenylpropyl)malononitrile was higher than that of other products. Hence, the substituents on the aromatic ring significantly influenced the product yields. The highest yield (70%) was of the unsubstituted chalcone (1a), suggesting that the absence of electron-donating or -withdrawing groups favors cyclization. Electron-withdrawing groups showed varied effects: a nitro substituent (1f) gave a relatively high yield (60%), while halogen substituents gave lower yields, in the order Cl (1c, 45%) > F (1b, 31%) > Br (1d, 26%). Meanwhile, the electron-donating methyl group (1e) resulted in a moderate yield (32%). Both steric and electronic effects of the substituents

strongly influence the efficiency of this transformation, with smaller, strongly electron-withdrawing groups generally enhancing reactivity compared to bulky or weakly donating substituents.

The proposed reaction mechanism is shown in Figure 10. Malononitrile is assumed to first protonate, forming the imino species. Further, the protonated chalcone at the carbonyl group activates the C=C bond, enabling the nucleophilic attack of the imino intermediate to form the enone intermediate. After obtaining the enone intermediate, a proton is lost from the catalyst and converted into the Michael adduct through enol-keto tautomerization.

Moreover, the scalability of the reaction was investigated by increasing the substrate concentration from 1 to 10 mmol under the optimized conditions. As seen in Figure 11, even at the 10 mmol scale, the desired product was formed constantly, with a yield of 70% comparable to that obtained from the 1-mmol-scale reaction.

An important feature of the CS-SO<sub>3</sub>H catalyst is its recyclability. The recovery process is extremely straightforward: it requires only filtration and washing with a suitable solvent. When the catalyst was recovered and reused in successive reactions, only a

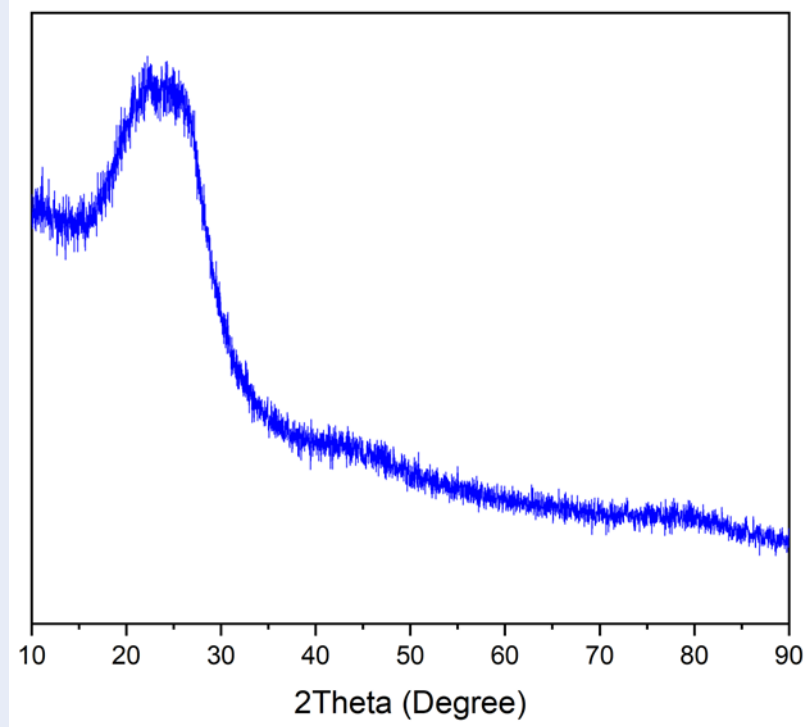


Figure 4: XRD pattern of CS-SO<sub>3</sub>H. [Source: Authors']

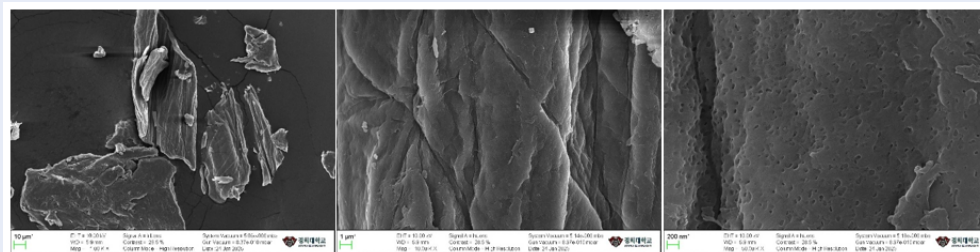


Figure 5: SEM images of CS-SO<sub>3</sub>H. [Source: Authors']

trivial decrease in isolated yield was observed relative to the first run, indicating remarkable reusability. After operating continuously for five reaction cycles, the catalyst maintained high efficiency relative to its initial value, as shown in Figure 12. The recovered catalyst was then characterized using FT-IR spectroscopy, as shown in Figure 13. The resulting spectra show that the characteristic absorption bands of the fresh catalyst remained unchanged, ensuring the structural durability and stability of the material for repeated use. The FT-IR spectrum of the recovered catalyst showed the same absorption bands as the fresh catalyst, such as a broad absorption band at 3323  $\text{cm}^{-1}$  corresponding to the -OH group, 1162  $\text{cm}^{-1}$

assigned to S=O stretching, and a band at 662  $\text{cm}^{-1}$  characteristic of O=S=O vibrations.

SEM analysis revealed that the recovered catalyst predominantly retains a bulk morphology, with pores of various sizes distributed on the surface (Figure 14). Moreover, comparison with the fresh catalyst shows no significant morphological differences, indicating that its structural integrity is maintained after use and that it can be reused over multiple catalytic cycles.

The EDS analysis showed that the synthesized catalyst contains 51.23 wt% C, 40.71 wt% O, 5.34 wt% N, and 2.72 wt% S. The corresponding atomic percentages were determined to be 58.64% C, 34.95% O, 5.24% N, and 1.13% S (Figure 15). The EDS analysis

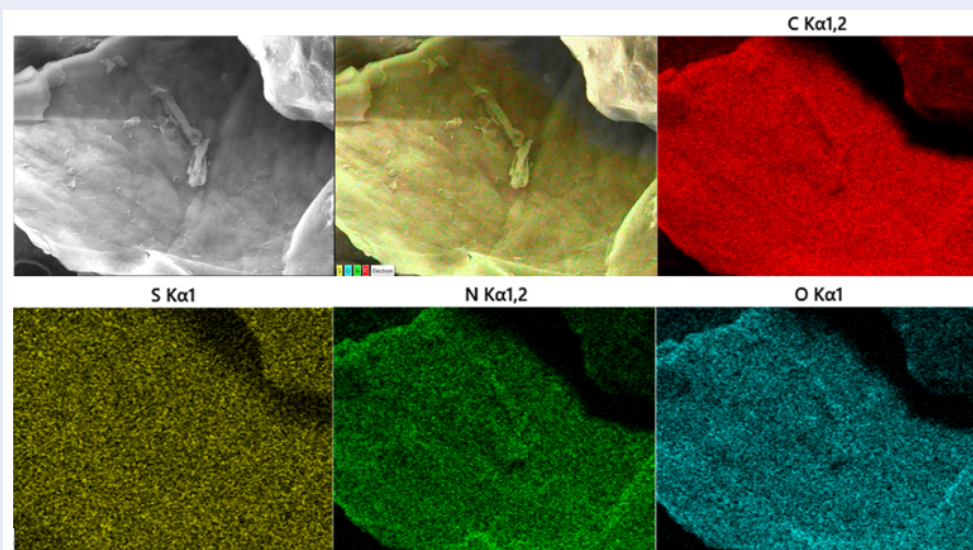


Figure 6: EDS maps of CS-SO<sub>3</sub>H. [Source: Authors']

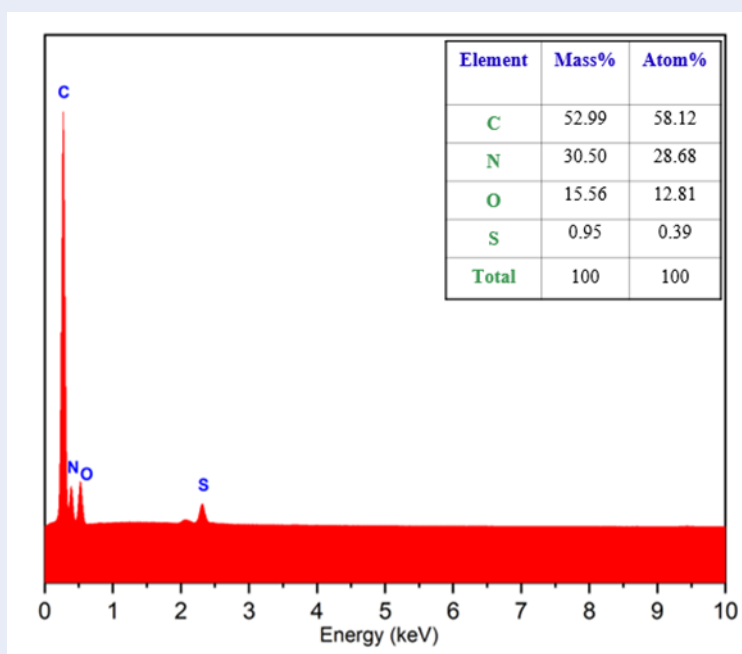


Figure 7: EDS of CS-SO<sub>3</sub>H. [Source:Authors']

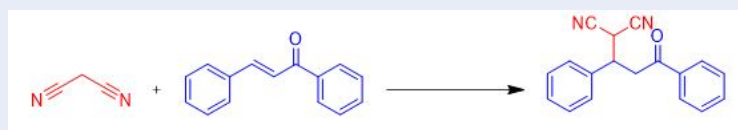


Figure 8: Synthesis of the 2-(3-oxo-1,3-diphenylpropyl)malononitrile scaffold (1a). [Source: Authors']

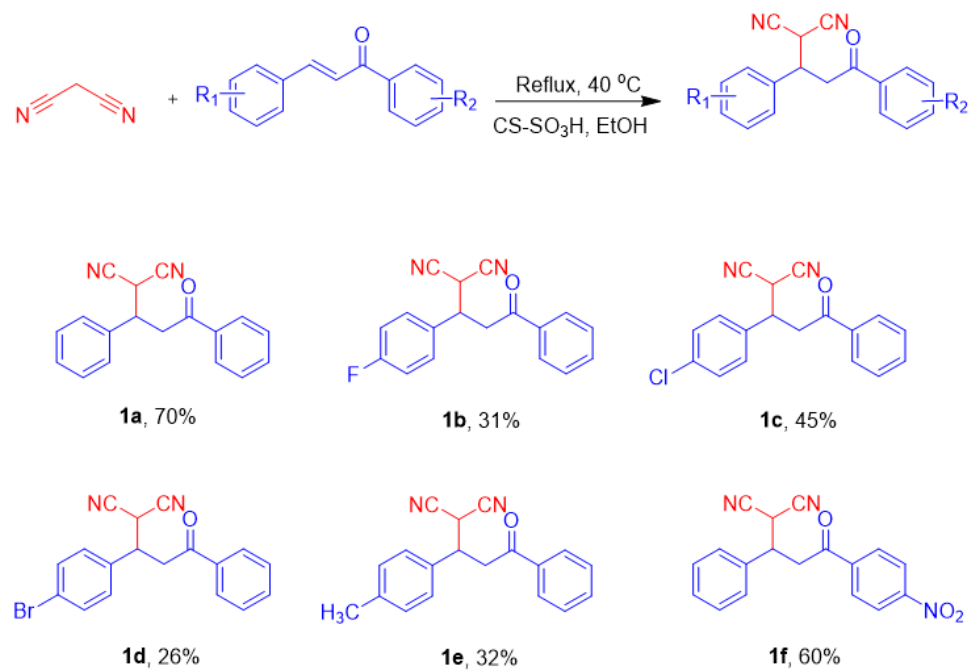


Figure 9: Scope of 2-(3-oxo-1,3-diphenylpropyl) malononitriles. [Source: Authors']

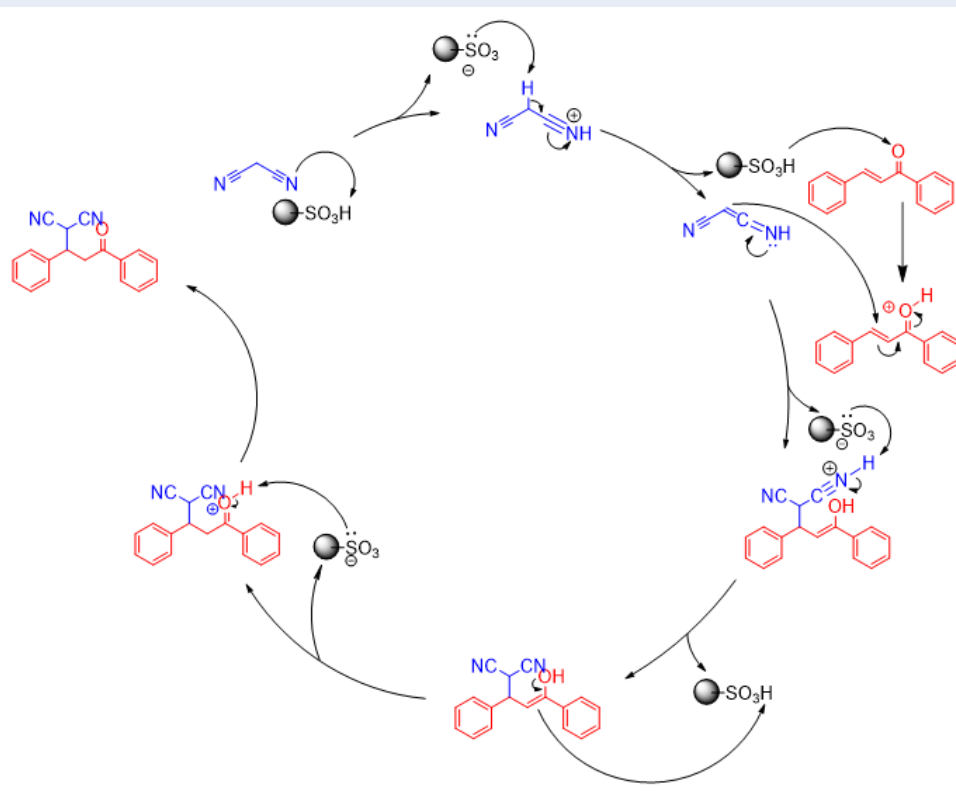


Figure 10: Proposed reaction mechanism. [Source: Authors']

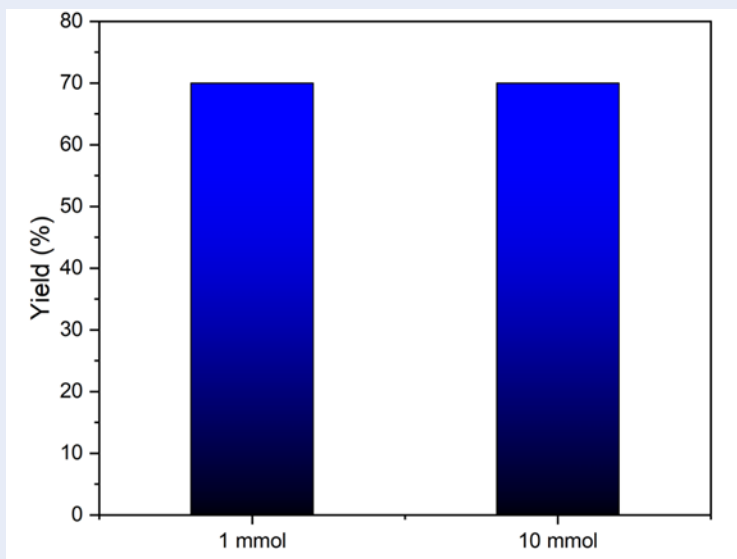


Figure 11: Scale-up experiment with 1 mmol and 10 mmol. [Source: Authors']

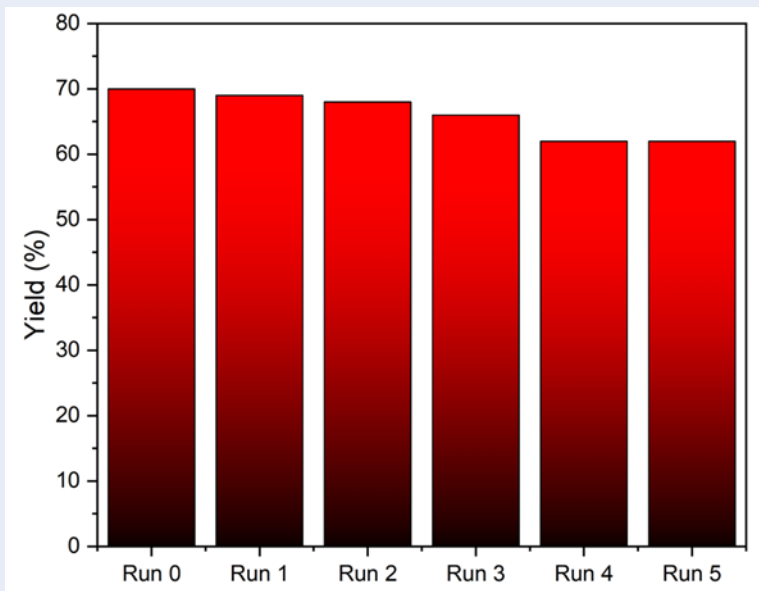


Figure 12: Reaction yield obtained after multiple recovery and reuse cycles of CS-SO<sub>3</sub>H catalyst. [Source: Authors']

shows that a high sulfur content is retained in the recovered catalyst, indicating that the catalyst may preserve its catalytic functionality and remain suitable for further reuse.

Control experiments were conducted by reacting chalcone or malononitrile individually in the presence of the catalyst. In the absence of both substrates and the catalyst, no product formation or side products were detected. When only a single substrate was

subjected to the catalytic conditions, only the corresponding starting material was observed. These results demonstrate that the concurrent presence of both substrates and the catalyst is essential for the reaction to proceed. Accordingly, the proposed reaction mechanism is tentative and provided solely as a plausible pathway for discussion.

To further study the role of the catalyst under the optimized reaction conditions, a control experiment was

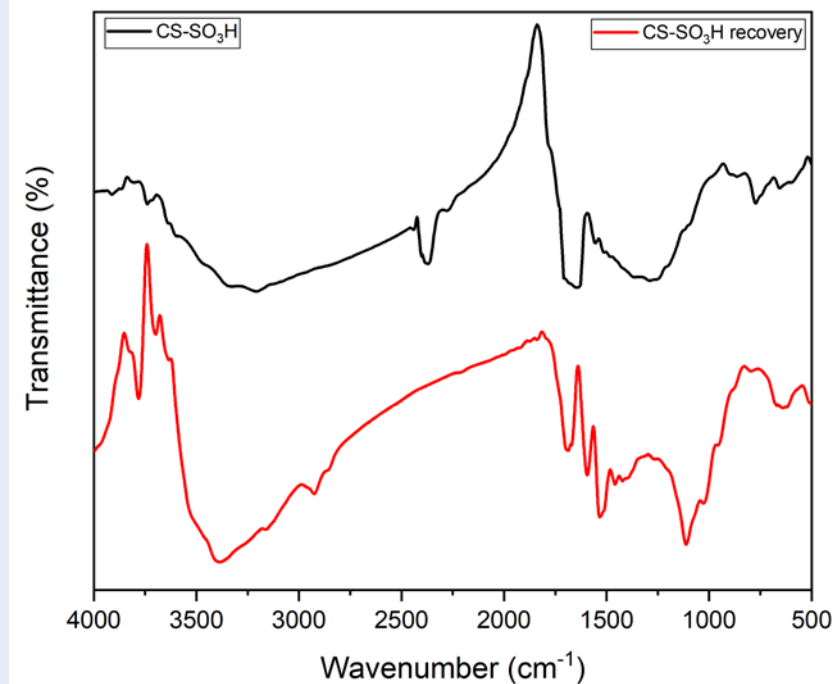


Figure 13: FT-IR spectra of CS-SO<sub>3</sub>H and recovered CS-SO<sub>3</sub>H. [Source: Authors']

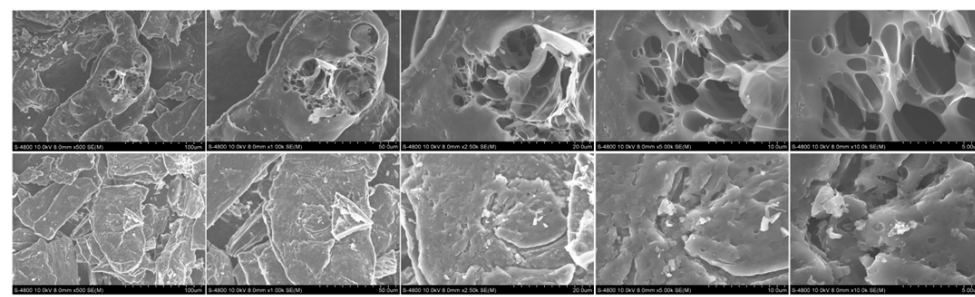


Figure 14: SEM images of recovered CS-SO<sub>3</sub>H. [Source: Authors']

conducted using chalcone (3 mmol) and malonitrile (3 mmol) with CS-SO<sub>3</sub>H (21 mg) at 40 °C in 9.0 mL of ethanol under magnetic stirring (Figure 16). The reaction was closely monitored and was divided into three stages. In Stage 1, the reaction was allowed to run for 60 minutes under the optimized experimental conditions, and it had a 33% yield after the catalyst was removed and the product was crystallized. In stage 2, the reaction was allowed to continue under identical conditions, with a yield of 47% after catalyst separation and removal, consistent with the progressive conversion observed in stage 1. In stage 3, the reaction was allowed to run for the entire 60 minutes with the catalyst present, and the yield after filtration

and crystallization was 65%, indicating the catalytic capacity of the optimized protocol.

Compared to previous studies, the present work demonstrates milder reaction conditions, a simpler catalyst for recovery and reuse, and a more environmentally friendly solvent (ethanol), while achieving relatively high yields of ~70%. As summarized in Table 4, previous catalysts generally required large volumes (e.g., 400 mg of Baker's yeast or 5–10% mol metal-based catalysts), long reaction times (1080–4800 min), and non-green solvents, such as CCl<sub>4</sub>, toluene, and CH<sub>2</sub>Cl<sub>2</sub>. In contrast, our CS-SO<sub>3</sub>H catalyst achieves a comparable yield (70%) using only 7 mg of catalyst under mild conditions (40 °C, 120 min)

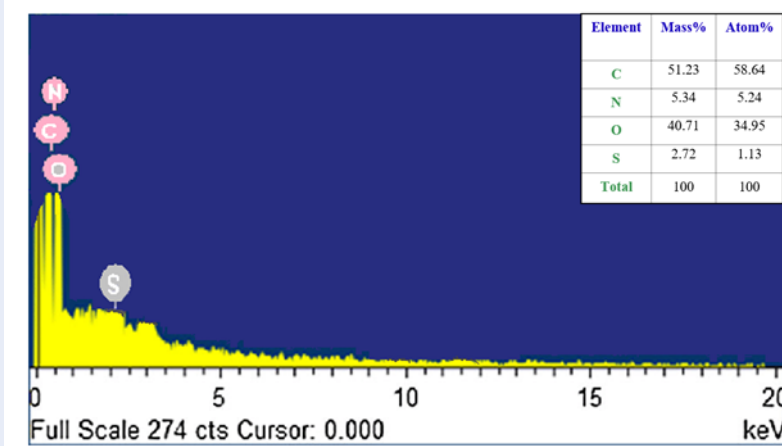


Figure 15: EDS results of recovered CS-SO<sub>3</sub>H. [Source:Authors']

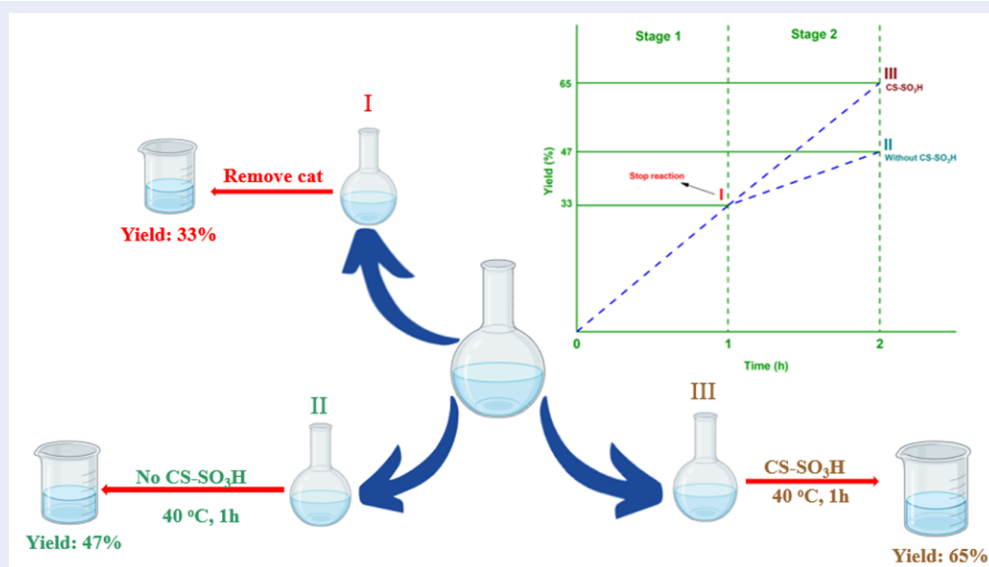


Figure 16: Leaching test results. [Source: Authors']

Table 4: Comparison with previously reported studies. [Source: Authors'] and [13,14,15,16]

Entry	Catalyst	Amount	Temp (°C)	Time (min)	Solvents	Yield (%)
1	Baker's yeast	400 mg	RT	1080	EtOH	52–85 <sup>13</sup>
2	PANQNF	5% mol	15	4320	CCl <sub>4</sub>	23–99 <sup>14</sup>
3	1b-Al(OiPr) <sub>3</sub>	10% mol	0	4800	Toluene	72–97 <sup>15</sup>
4	Catalyst V	10% mol	r.t	2160	CH <sub>2</sub> Cl <sub>2</sub>	87 <sup>16</sup>
5	CS-SO <sub>3</sub> H	7 mg	40	120	EtOH	70 (This work)

in ethanol, a greener solvent. Additionally, CS-SO<sub>3</sub>H is easy to prepare and exhibits excellent reusability, highlighting the novelty and practical advantages of our system over previously reported methods.

## CONCLUSION

The results of this study corroborated the activity of the CS-SO<sub>3</sub>H catalyst toward Michael addition of chalcone and malononitrile at mild temperatures (40 °C, 2 h) in ethanol. In general, CS-SO<sub>3</sub>H with Brønsted acid sites was produced to serve as a green, reusable catalyst. The benefits of this system include shorter reaction times than in earlier studies, an environmentally friendly solvent, a recyclable catalyst, and stable yields of up to 70%.

## LIST OF ABBREVIATIONS

*p*-TSA: *p*-Toulenesulfonic acid  
EtOH: Ethanol  
MeOH: Methanol  
CS: Chitosan  
NMR: Nuclear Magnetic Resonance  
DMSO: Dimethyl sulfoxide  
RT: Room temperature

## ACKNOWLEDGEMENTS

We acknowledge Ho Chi Minh City University of Science (HCMUS), VNU-HCM for supporting this study.

## CONFLICT OF INTEREST STATEMENT

The authors declare that they have no conflict of interest.

## AUTHOR CONTRIBUTIONS

**Duong Trinh The Anh:** investigation, methodology, resources, formal analysis, validation, data curation, and writing – original draft. **Nguyen Truong Hai:** methodology, resources, formal analysis, validation, data curation, writing – original draft, writing – review and editing, and supervision.

## REFERENCES

- Gupta P, Paul S. Solid acids: green alternatives for acid catalysis. *Catalysis Today*. 2014;236:153–70. Available from: <https://doi.org/10.1016/j.cattod.2014.04.010>.
- Si YF, Chen XL, Fu XY, Sun K, Song X, Qu LB, et al. Divergent g-C<sub>3</sub>N<sub>4</sub>-catalyzed Reactions of Quinoxalin-2(1H)-ones with N-Aryl Glycines under Visible Light: Solvent-Controlled Hydroaminomethylation and Annulation. *ACS Sustainable Chemistry; Engineering*. 2020;8(29):10740–6. Available from: <https://doi.org/10.1021/acssuschemeng.0c02289>.
- Muhammad MH, Chen XL, Liu Y, Shi T, Peng Y, Qu L, et al. Recyclable Cu@C<sub>3</sub>N<sub>4</sub>-Catalyzed Hydroxylation of Aryl Boronic Acids in Water under Visible Light: Synthesis of Phenols under Ambient Conditions and Room Temperature. *ACS Sustainable Chemistry; Engineering*. 2020;8(7):2682–7. Available from: <https://doi.org/10.1021/acssuschemeng.9b06010>.
- Li W, Liu Y, Wang B, Song H, Liu Z, Lu S, et al. Kilogram-scale synthesis of carbon quantum dots for hydrogen evolution, sensing and bioimaging. *Chinese Chemical Letters*. 2019;30(12):2323–7. Available from: <https://doi.org/10.1016/j.ccllet.2019.06.040>.
- Gao F, Zhang S, Lv Q, Yu B. Recent advances in graphene oxide catalyzed organic transformations. *Chinese Chemical Letters*. 2022;33(5):2354–62. Available from: <https://doi.org/10.1016/j.ccllet.2021.10.081>.
- Gao X, Chen X, Zhang J, Guo W, Jin F, Yan N. Transformation of Chitin and Waste Shrimp Shells into Acetic Acid and Pyrrole. *ACS Sustainable Chemistry; Engineering*. 2016;4(7):3912–20. Available from: <https://doi.org/10.1021/acssuschemeng.6b00767>.
- No HK, Meyers SP. Preparation and Characterization of Chitin and Chitosan—A Review. *Journal of Aquatic Food Product Technology*. 1995;4(2):27–52. Available from: [https://doi.org/10.1300/J030v04n02\\_03](https://doi.org/10.1300/J030v04n02_03).
- Kumar MNR. A review of chitin and chitosan applications. *Reactive (& Functional Polymers*. 2000;46(1):1–27. Available from: [https://doi.org/10.1016/S1381-5148\(00\)00038-9](https://doi.org/10.1016/S1381-5148(00)00038-9).
- Xie Q, Yang X, Xu K, Chen Z, Sarkar B, Dou X. Conversion of biochar to sulfonated solid acid catalysts for spiramycin hydrolysis: insights into the sulfonation process. *Environmental Research*. 2020;188. Available from: <https://doi.org/10.1016/j.envres.2020.109887>.
- Zhang T, Li W, Jin Y, Ou W. Synthesis of sulfonated chitosan-derived carbon-based catalysts and their applications in the production of 5-hydroxymethylfurfural. *International Journal of Biological Macromolecules*. 2020;157:368–76. Available from: <https://doi.org/10.1016/j.ijbiomac.2020.04.148>.
- Zheng B, Chen L, He L, Wang H, Li H, Zhang H, et al. Facile synthesis of chitosan-derived sulfonated solid acid catalysts for realizing highly effective production of biodiesel. *Industrial Crops and Products*. 2024;210. Available from: <https://doi.org/10.1016/j.indcrop.2024.118058>.
- Wang J, Huang L, Cheng C, Li G, Xie J, Shen M, et al. Design, synthesis and biological evaluation of chalcone analogues with novel dual antioxidant mechanisms as potential anti-ischemic stroke agents. *Acta Pharmaceutica Sinica B*. 2019;9(2):335–50. Available from: <https://doi.org/10.1016/j.apsb.2019.01.003>.
- Punyapreddiwar ND, Zodape SP, Wankhade AV, Pratap UR. Conjugate addition of malononitrile on chalcone: biocatalytic CC bond formation. *Journal of Molecular Catalysis B, Enzymatic*. 2016;133:124–6. Available from: <https://doi.org/10.1016/j.molcatb.2016.08.004>.
- Zhang Y, Zhang H, Liu J, Tao M, Ma N, Zhang W. Heterogeneous fiber-based asymmetric quinine catalyst for highly enantioselective Michael addition and tandem cyclization to 4H-pyrans. *Chemical Engineering Journal*. 2023;469. Available from: <https://doi.org/10.1016/j.cej.2023.143928>.
- Shi J, Wang M, He L, Zheng K, Liu X, Lin L, et al. Enantioselective Michael addition of malononitrile to chalcones catalyzed by a simple quinine-Al(Oi)Pr(3) complex: a simple method for the synthesis of a chiral 4H-pyran derivative; 2009. Available from: <https://doi.org/10.1039/b908632c>.
- Lin N, Wei QX, Jiang LH, Deng YQ, Zhang ZW, Chen Q. Asymmetric Michael Addition of Malononitrile with Chalcones via Rosin-Derived Bifunctional Squaramide. *Catalysts*. 2020;10(1):14. Available from: <https://doi.org/10.3390/catal10010014>.